Int. J. Electrochem. Sci., 16 **(2021)** Article Number: 211147, doi: 10.20964/2021.11.50

International Journal of
ELECTROCHEMICAL
SCIENCE
www.electrochemsci.org

Corrosion Behavior of Au Coating on 316L Bipolar Plate in Accelerated PEMFC Environment

Chen Wen[1,2], *Junwei An*[1,3,*], *Jimin Hua*[3], *Xiaoting Lv*[3], *Liangxi Ding*[1], *Xiaolin Qiu*[1],

[1] Nanchang Institute of Technology, Nanchang, Jiangxi, 311033, China;
[2] Beijing Spacecrafts, China Academy of Space Technology, Beijing, 100190, China
[3] Inner Mongolia Qingmeng New Materials Co., Ltd., Inner Mongolia Municipality, 013560, China
[*]E-mail: 15810532852@126.com

Received: 17 May 2021 / *Accepted:* 12 September 2021 / *Published:* 10 October 2021

The material Au has high conductivity and good corrosion resistance, which is benefit for proton exchange membrane fuel cells (PEMFC) application. In order to evaluate the corrosion performance of Au coating for PEMFC applications, the electrochemical corrosion behaviors in 0.5 M H_2SO_4 with 10 ppm of fluoride ions at 80 ℃were investigated by potentiodynamic polarization (PP) tests. And the corrosion characteristics were characterized by using SEM, EDX, XRD and XPS methods. The results showed that as the experiment time increases from 0 h to 48 h, the self-corrosion current increases from 1.716×10^{-5} A/cm^2 to 2.243×10^{-4} A/cm^2. As the reaction develops, the corrosion rate of the Au coating in accelerated PEMFC environment increases. Combined with the morphologies and corrosion products analysis, and also electrochemical impedance spectroscopy (EIS), the corrosion mechanisms were discussed.

Keywords: Au Coating, Corrosion, Electrochemical, PEMFC

1. INTRODUCTION

Proton exchange membrane fuel cells (PEMFC) have been widely developed as the key new power source with the high output power density and the only product water [1-3]. Bipolar plate is one of the most important part for providing the electrical connectivity between cells, and separating the cathode and anode reactant gases. The bipolar plate substantially impacts the weight of PEMFC, so the super thin metal bipolar is considered as the ideal material for weight reduction [4,5].

With high mechanical properties, high electrical conductivity and low cost, 316L steels are investigated widely as the bipolar plate for PEMFC. However, the main problems for 316L bipolar plate are passivation and corrosion resistance [6,7]. Many researchers have tried to improve the property combined conductivity and corrosion resistance, such as heat treatment, strain, coatings, and so on [8-

11]. Dong [12] demonstrated that the Cr/N co-doped DLC film (with Cr target power of 90 W) has outstanding performance in both electrical conductivity and corrosion resistance. Mo doped CrN coating can obviously improve the corrosion resistance of samples [13]. Mani Studied the corrosion behavior of 316L steel in 0.5 M H_2SO_4 with 2 ppm of fluoride ions at 80 ℃ and found that corrosion protection performance is in the order of TiAlN < 316L SS < TiN/TiAlN < TiN[14].

In this paper, the corrosion behaviors of Au coating were investigated in accelerated environment of proton exchange membrane fuel cell in 0.5 M H_2SO_4 with 10 ppm of fluoride ions at 80℃. The corrosion properties with time were evaluated by electrochemical methods. Combined with the morphologies and characteristics of corrosion products, the corrosion mechanism was discussed.

2. EXPERIMENTAL

2.1 Specimens

Commercial 316L were cut into specimens of 30 mm ×30 mm × 0.1 mm by laser cutting as the substrate material. The specimens were treated by hot calibration to maintain flatness and then cleaned by using ethanol in ultrasonic cleaner and dried by compressed air at room temperature.

The Au coating procedure was carried out. The Cu transition layer was deposited between 316L plates and Au coating by electrochemical methods with thickness about 10 μm. And then the Au coating was plated for the thickness about 1 μm. After plating, the specimens were dried at 100 ℃ in the vacuum oven for 2 h.

2.2 Corrosion tests

The corrosion performance was tested by immersing the specimens in accelerated simulated PEMFC environment (0.5 M H_2SO_4 +10 ppm HF solution at 80 ℃) for different time. And then the specimens with different immersion time were evaluated by electrochemical methods in the same accelerated simulated PEMFC environment (0.5 M H_2SO_4 +10 ppm HF solution at 80 ℃).

2.3 Characterization

After the process of immersion, the micro morphology was detected by field emission scanning electron microscope (FESEM) in combination with energy dispersive X-ray analysis spectrometer (EDS), and the element composition and content were characterized by EDS. The phase composition of Ag bipolar plate was characterized by X-ray diffraction (XRD) with the instrument operating at 40 kV and 40 mA X-ray photoelectron spectroscopy (XPS) was used to analyze the chemical and binding energy states of the Au layer.

After different immersion time for 0 h, 12 h, 24 h, 48 h, the electrochemical measurements were performed by using a conventional three-electrode electrochemical cell on a CHI electrochemical system with a 23Co14Ni12Cr3Mo of 1 cm^2 as working electrode. A large platinum used as the counter electrode.

A saturated calomel electrode (SCE) was used and all potentials were referred to this electrode. All electrochemical experiments were performed in the same accelerated simulated PEMFC environment (0.5 M H_2SO_4 +10 ppm HF solution at 80 ℃). The open circuit potential (OCP) tests were carried out by potentiostat mode for 3600 s to reach the steady potential. And then the EIS was tested from 100 kHz~10 mHz, the dada was simulated by Zsimpwin software. The potentiodynamic polarization (PP) tests were scanned from -0.5 V~0.5 V(vs.ocp) at the rate of 5 mV/s.

3. RESULTS AND DISCUSSION

3.1 Potentiodynamic Polarization Test

The corrosion rate were evaluated by polarization methods in solution of 0.5 M H_2SO_4+10 ppm HF at 80 ℃， and the results are given in figure 1 and table 1. It can be seen that the self-corrosion potential increases with the increasing immersion time, but the self-corrosion potential immersed for 12 h in the solution lower than that of without immersion. It indicates that the electrochemical reactions happen when the specimens immerse in the solution, meanwhile, a film is gradually formed which prevent the corrosion trend.

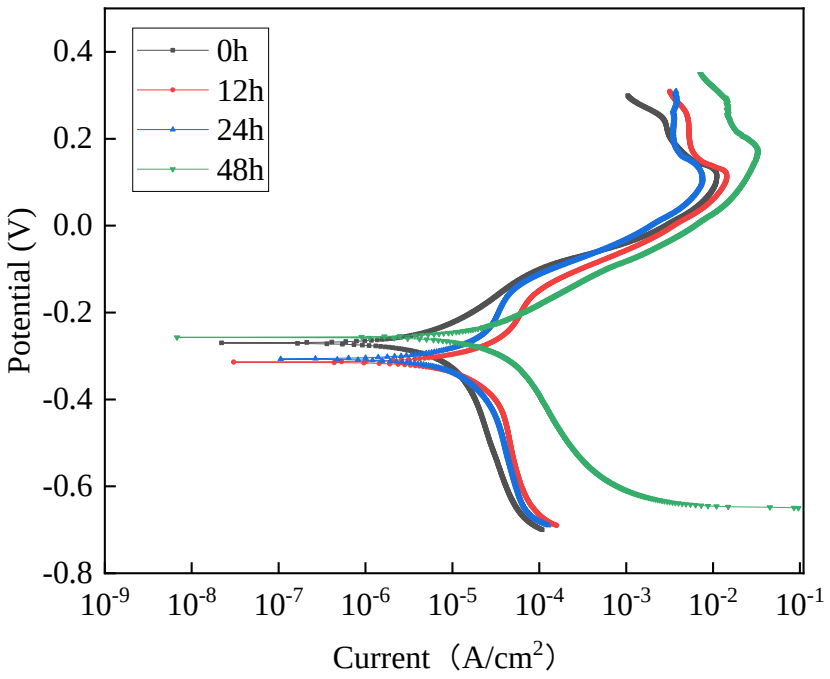

Figure 1. The Potentiodynamic polarization curves of Au coating with different immersion time in accelerated simulated PEMFC environment

As the experiment time increases from 0 h to 48 h, the self-corrosion current increases from 1.716×10^{-5} A/cm^2 to 2.243×10^{-4} A/cm^2, which shows that as the reaction develops, the corrosion rate increases. H. Q. Fan[15] prepared a composite coating by introducing Au microdots onto TiN coated stainless steel (Au/TiN/SS), which shows that Au/TiN/SS has a corrosion potential of 0.178 V,

respectively. At the normal working potential in the cathode of PEMFCs, the anodic Corrosion Current of Au/TiN/SS is 1.6×10^{-4} mA/cm^2. The corrosion potential of the Au/TiN/SS coating is higher than that of the Au coating without immersion corrosion, but the corrosion current of the film is lower than that of the Au coating after 48 h of immersion. D. G. Liu[16] also did similar research, prepared Cu-Ni-Au film on diamond/Cu composite and tested the corrosion resistance of the film. The result shows that Cu-Ni-Au multilayer coatings can provide the excellent corrosion resistance properties. The corrosion current of the film is 1.3×10^{-3} A/cm^2 and the corrosion potential of the film is about 0.914 V. Based on the above situation, the Au coating prepared in this experiment has good corrosion resistance compared with other Au films that have been researched.

Table 1. The fitted results of potentiodynamic polarization curves

Time(h)	Corrosion Potential(V)	Corrosion Current(A/cm^2)
0	-0.278	1.716×10^{-5}
12	-0.335	3.757×10^{-5}
24	-0.324	4.169×10^{-5}
48	-0.256	2.243×10^{-4}

3.2 Morphology of Au coating

In order to find out the mechanism of self-corrosion potential change, the immersed specimens were characterized. The morphologies of Au coating for different corrosion time of SEM is shown in Figure 1. And the element compositions of the specimens where zone scanned are given in Table 2. It can be seen that the Au coating shows flat surface with particles on the surface. When immersed in the solution of 0.5 M H_2SO_4+10 ppm HF at 80 ℃, the surface becomes rough with some nano pit pores. The corrosion condition of the Au coating is a high temperature environment, so the reason for the corrosion pits may be the thermal aging of the film[17], which accelerates the corrosion of the film.With the immersion time going on, the surface appears some corrosion sign. From the EDS results, After immersing in the etching solution for 12 h, S and F elements were detected on the surface of the film, indicating that the elements in the etching solution have penetrated into the film at this time. With the extension of the immersion time, the content of Au element decreases, indicating that the content of the film is mainly Au. As the corrosion time increases, the Au component in the film is consumed. The content of S and F elements increased, indicating that S and F elements accelerated the corrosion process. The increase in O element content may be involved in the formation of corrosion products.

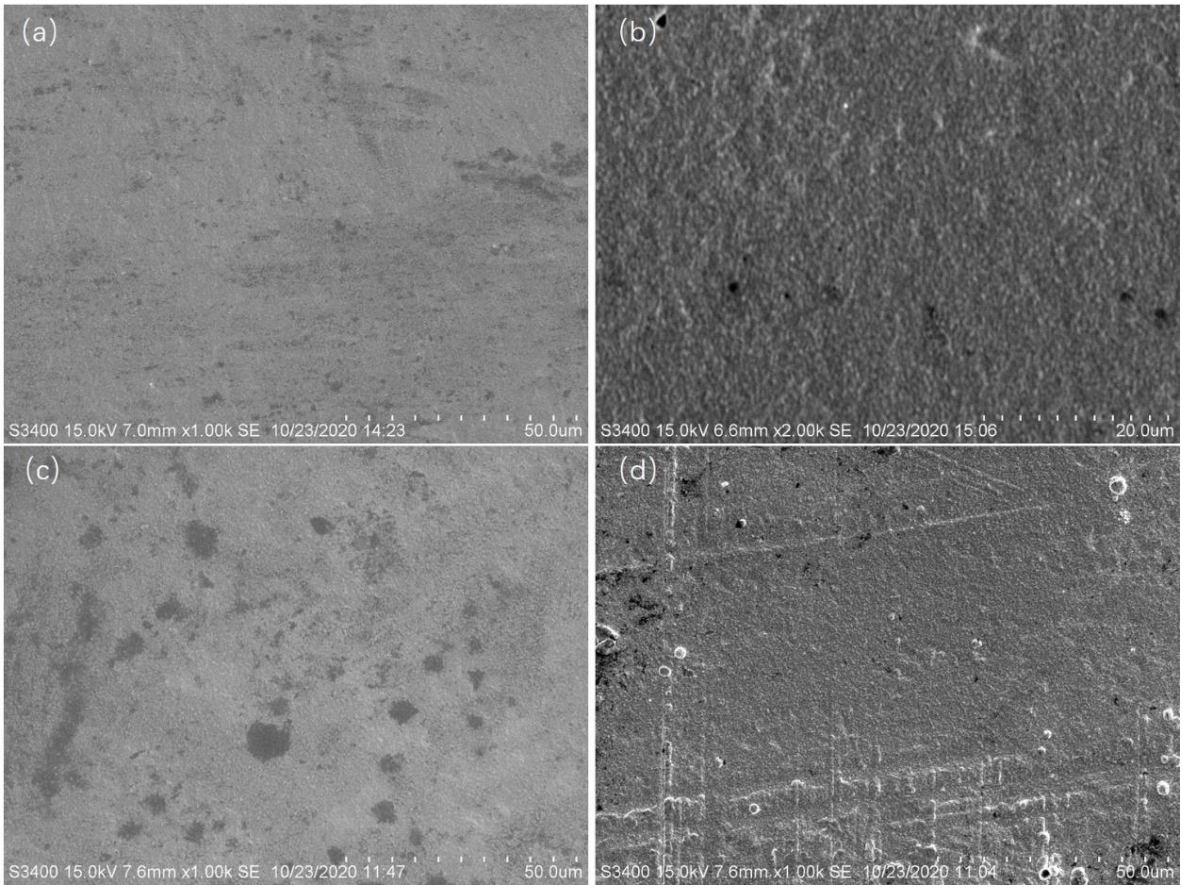

Figure 2. SEM morphologies of Au coating with different immersion time in accelerated simulated PEMFC environment. (a) 0 h, (b) 12 h, (c) 24 h, (d) 48 h

Table 2. the element compositions of the Au coating specimens with different immersion time in accelerated simulated PEMFC environment (wt%)

Time(h)	Au	O	S	F
0	98.68	1.32	0	0
12	96.47	3.45	0.03	0.05
24	91.58	6.39	1.02	1.01
48	86.22	8.76	3.25	1.77

The XRD and XPS curves with and without immersion are shown in figure 3 and figure respectively. It can be seen from the XRD results that the surface material mainly contains Au, which is consistent with EDS results. There are no S peaks or F peaks in the XRD results, and only small O peaks for 48 h, which demonstrated that the corrosion of the Au coating is slight and further proved the good corrosion resistance of Au coating. Compared to the EDS results that with the immersion time increases, the elements of O, S and F increase, which demonstrates that the corrosion products are mainly composed of Au_2O_3.

From the XPS results can be seen that the specimens without immersion show Au 4f peak and C 1s peak, meanwhile, the immersed specimens present O 1s peak. As the results above, it can be found

that when immersed in 0.5 M H_2SO_4+10 ppm HF solution, the heavy corrosive environment accelerates corrosion, leading to self-corrosion potential reduction immediately, but as the immersion time increases, the local area of Au coating forms films which mainly contains Au and O. The formation of Au_2O_3 reduces corrosion trend, leading to self-corrosion potential increasing with the increasing immersion time.

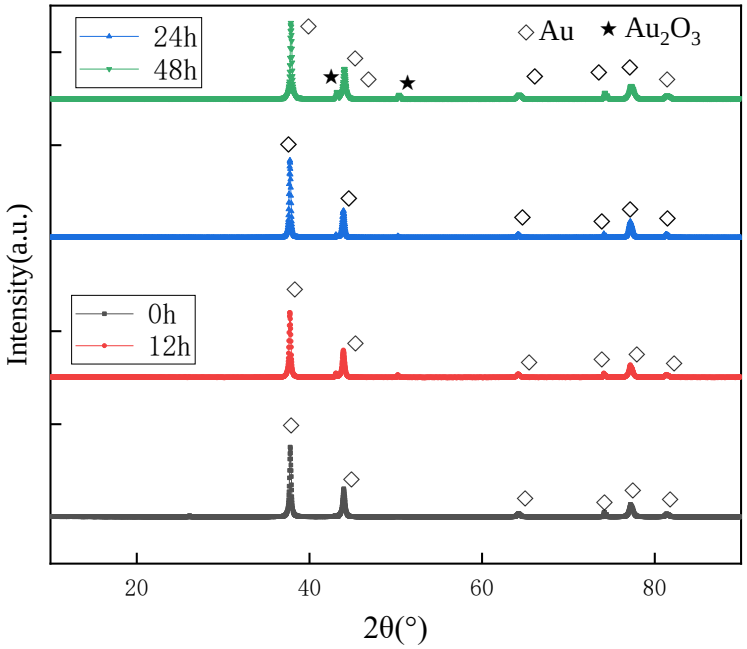

Figure 3. the XRD curves of the Au coating with different immersion time in accelerated simulated PEMFC environment

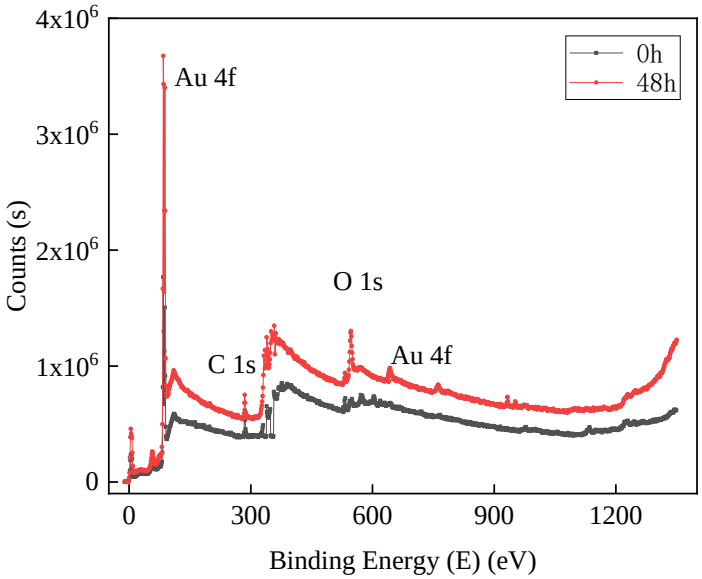

Figure 4. the XPS results of the Au coating before and after immersion in accelerated simulated PEMFC environment

3.3 EIS measurements

In order to find out the mechanism of the self-corrosion current change, the electrochemical impedance spectroscopy (EIS) were tested and the curves are given in figure 5, and also the fitting data by using the equivalent circuit model R(Q(RW))(QR) as figure 6 are given and table2, respectively. From the Nyquist phase can be seen that all the specimens can be divided to two areas. The high frequency region has a time constant capacitive reactance arc, and the low frequency region is an obvious characteristic of diffusion control. It can be seen that as the immersion time increases from 0h to 48h, the reaction resistance of the specimens decreases from 3774 Ωcm^2 to 1487 Ωcm^2, which indicates that the corrosion resistance reduces with the increasing immersion time, consisted with the self-corrosion current results. Because the disbonding range and the gap increase, this creates more conditions for crevice corrosion (anode corrosion), and the cathode current shielding effect is intensified [18, 19]. Due to the corrosive environment of H^+, SO_4^{2-} and F^-, the electrochemical reactions happen in the Au surface and pit pores forms, which accelerates the corrosion rate, consistent with literature results [20-22]. The gold (Au) coating can form a barrier layer which improve the corrosion resistance of the substrate [23-24].

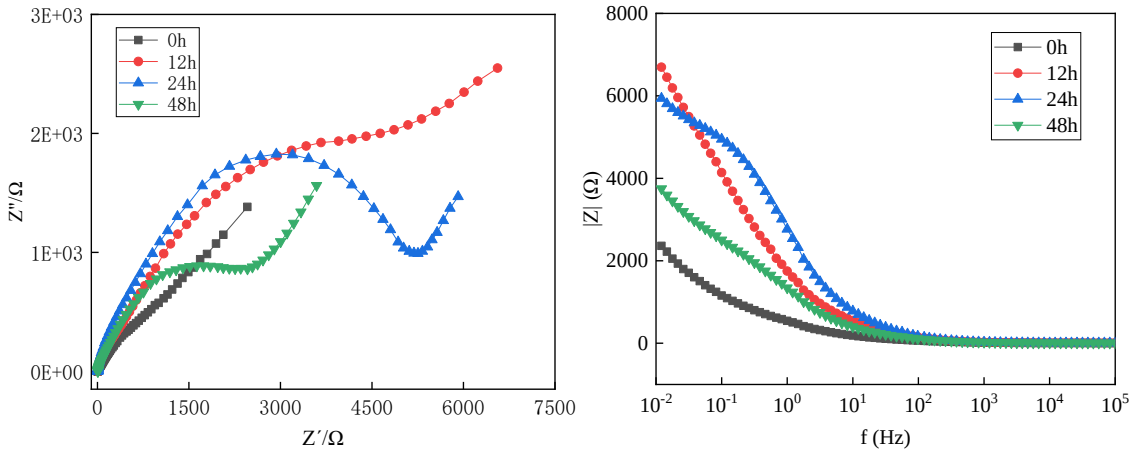

Figure 5. The EIS curves of the Au coating with different immersion time in accelerated simulated PEMFC environment, (a) Nyquist plots, (b) Bode plots

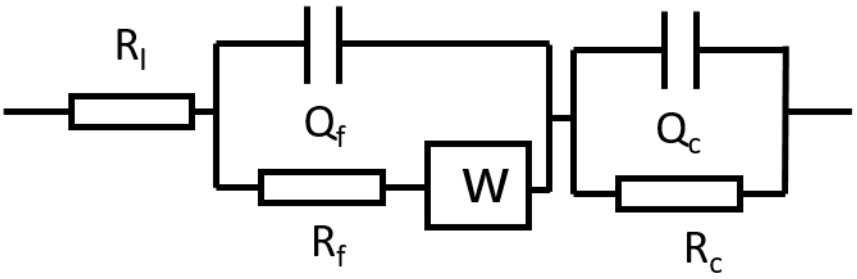

Figure 6. Equivalent circuit model of EIS results, (R_l stands for solution resistance, Q_f and R_f are electric double layer capacitance and resistance respectively, Q_c and R_c are reaction capacitance and resistance respectively. W is the warburg resistance. Q is a constant phase angle element)

However, the F ion causes pitting corrosion of coatings contains Au, and the corrosion is accelerated by the F ions [25]. The corrosion pit can bring additional sulfates into the pit and result in

serious damage [26]. The Cu transition layer was electrodeposited between 316L plates and Au coating in this experiment by electrochemical methods with thickness about 10 μm. The conductivity of Au is similar to that of Cu and Au is more chemically stable and not easy to oxidize compared to Cu, so the impedance of Au-coated ceramic-lined chamber is theoretically very close to that of Cu-coated ceramic-lined chamber[27]

Table 2. The fitting results of EIS spectra by Zsimpwin software

Time	$R_l(\Omega cm^2)$	Q_f ($\Omega^{-1}s^n cm^2$)	n	$R_f(\Omega cm^2)$	$W(S\cdot sec^{0.5}/cm^2)$	Q_c ($\Omega^{-1}s^n cm^2$)	n	$R_c(\Omega cm^2)$
0h	4.39	3.669×10^{-5}	0.891	3774	1.760×10^{-3}	6.450×10^{-4}	0.661	5440
12h	7.56	2.662×10^{-5}	0.800	2796	1.123×10^{-3}	1.883×10^{-4}	0.689	4977
24h	5.74	2.773×10^{-5}	0.924	1869	2.195×10^{-3}	6.959×10^{-5}	0.812	4398
48h	5.48	1.375×10^{-5}	0.666	1487	1.873×10^{-3}	1.282×10^{-4}	0.995	876.5

4. CONCLUSIONS

The corrosion behaviors of the Au coating were evaluated in accelerated PEMFC environment (0.5 M H_2SO_4+10 ppm HF at 80 ℃) and it can be concluded that:

(1) The immersion time increases from 0 h to 48 h, the reaction resistance of the specimens decreases from 3774 Ωcm^2 to 1487 Ωcm^2, the self-corrosion current increases from 1.716×10^{-5} A/cm^2 to 2.243×10^{-4} A/cm^2, which shows that as the reaction develops, the corrosion rate increases.

(2) The local area of Au coating forms films mainly contains Au and O reduces corrosion trend, leading to self-corrosion potential increasing with the increasing immersion time.

(3) Due to the corrosive environment of H^+, SO_4^{2-} and F^-, the electrochemical reactions happen in the Au surface and pit pores forms, accelerating the corrosion.

ACKNOWLEDGEMENTS
The authors acknowledge the financial support of the Science and Technology Research Project of Jiangxi Province (2018BBG78050).

References

1. H. C. Liu, W. M. Yang, J. Tan and L. S. Cheng, *Fuel Cells*., 19 (2019) 51.
2. J. Shen, L. P. Zeng, Z. C. Liu and W.Liu, *Heat Mass Transfer,* 55 (2019) 811.
3. G. Loreti, A.L. Facci, I. Baffo and S. Ubertini, *Appl. Energy*, 235 (2019) 747.
4. D. H. Wen, L. Z. Yin, Z. Y. Piao, C. D. Lu, G. Li, and Q. H. Leng, *Int. J. Heat Mass Transfer*, 121

(2018) 121.
5. D. H. Wen, L. Z. Yin, Z. Y. Piao, C. D. Lu, G. Li and Q. H. Leng, *Int. J. Energy Res.,* 41 (2017) 2184.
6. N. B. Huang, H. Yu, L. S. Xu, S. Zhan, M. Sun and D. W. Kirk, *Results Phys.*, 6 (2016) 730.
7. Y. L. Wang, S. H. Zhang, Z. X. Lu, L. S. Wang and W. H. Li, *Corros. Sci*., 142 (2018) 249.
8. D. G. Li, D. R. Chen and P. Liang, *Int. J. Hydrogen Energy*, 45 (2020) 30101.
9. J. J. Zhao, Z. K. Tu and S. H. Chan, *J. Power Sources*, 488 (2021) 229434.
10. C. P. Zhang, C. M. Hao, Y. T. Han, F. M. Du, H. Y. Wang, X. Y. Wang and J. C Sun, *Surf. Coat. Technol*., 397 (2020) 126064.
11. J. L. Lv, T. X. Liang and W. L Guo, *Int. J. Hydrogen Energy*., 40 (2015) 10382.
12. H. M. Dong, S. He, X. Z. Wang, C. Z. Zhang and D. Sun, *Diamond Relat. Mater.*, 110 (2020) 108156.
13. J. Jin, H. J. Liu, D. C. Zheng and Z. X. Zhu, *Int. J. Hydrogen Energy*, 43 (2018) 10048.
14. S. P. Mani, A. Srinivasan and N. Rajendran, *Int. J. Hydrogen Energy*, 40 (2015) 3359.
15. H. Q. Fan, D. D. Shi, X. Z. Wang, D , J. L. Luo, J. Y. Zhang, Q. Li, *Int. J. Hydrogen Energy*, 45(2020)29442-29448.
16. D. G. Liu, Y. J. Mai, J. Sun, Z. J. Luan, W. C. Shi, L. M. Luo, H. Lia, Y. C. Wu, *Ceram. Int.*, 43(2017)13133-13139.
17. Z. X. Chen, J. Hillaireta, V. Turq, Y. T. Song, R. Laloo, J. M. Bernarda, K. Vulliezd, G. Lombarda, C. Hernandez, Q. X. Yang, L. Ferreira, F. Fesquet, P. Mollard, R. Volpe, *Thin Solid Films*, 659(2018)81-88.
18. Q. Liu, W. Wu,Y. Pan, Z. Y.Liu, Constr. *Build. Mater.*, 20(2018) 622-633.
19. X. H. Wang, Q. Liu, Y. C. Chun, Y. C. Li, Z. Q. Wang, J. Mater. Eng. Perform., 27(2018) 3060-3071.
20. Y. Yang, L. J. Guo and H. T. Liu, *J. Power Sources*, 195 (2010) 5651.
21. Y. Yang, L. J. Guo and H. T. Liu, *Int. J. Hydrogen Energy*, 36 (2011) 1654.
22. Y. Yang, L. J. Guo and H. T. Liu, *Int. J. Hydrogen Energy*, 37 (2012) 1875.
23. Z. H. Huang, Y. J. Zhou and W. He, *Surf. Coat. Technol.*, 320 (2017) 126.
24. X. K. Zhang, Q. Y. Qian, L. Qiang, B. Zhang and J. Y. Zhang, *Microelectron. Reliab.*, 110 (2020) 113695.
25. S. A. Salhizadeh, I. Carvalho, R. Serra. S. Calderon V, P. J. Ferreira, A. Cavaleiro and S. Carvalho, *Surf. Coat. Technol*., 401 (2020) 126240.
26. L. Y. Zhao and Z. K. Kong, *19th ICEPT*., 1 (2018)1575.
27. C. C. Li, C. Luo, J. L. Liu, J. C. Yang, G. D. Shen, J. Meng, W. S. Yang, Y. Q. Yang, J. X. Wu, G. Y. Zhu, J. W. Xia, W.J. Xie, Z. Chai, X .J. Lina, X. L. Ma, X. P. Zhang, Y. P. Wan, J. Q. Jiao, X. R. Zhu, Y. M. Gao, Z. W. Niu, Z.S. Nie, Z. J. Hu, *Vacuum.*, 184 (2021) 109898.